研 究 解 説

Micro Optical Scanners of Photoresist Reflow Lens on MEMS XY-Stage

Hiroshi Toshiyoshi*, Guo-Dung John Su**, Jason LaCosse** and Ming C. Wu**

1. Introduction

Most optical crossconnectors (OXCs) for today's fiber networks are using opto-electric (OE) and electro-optic (OE) conversion of signals with high-speed electronics. This type of switch has very short media interrupting time of switching. However, they start to behave as a "bottleneck" to limit the bandwidth of traffic when the modulation rate exceeds the mobility of electron, which occurs at several tens of Gbps or beyond. On the other hand, "all-optical" switches refer to another type of OXCs which redirect optical signals from a fiber to another without going through OE-or EO-conversion. Conventional fiber optic switches using mechanical movable prisms or beam splitters are examples of all-optical OXC. Switching speed of mechanical OXC is generally slow in milliseconds to seconds range but their bandwidth is large enough to cover the whole range of optical fibers.

Microelectromechanical system (MEMS) technology provides new technologies to fill the gap between these two different types of OXCs [1, 2]. Tiny pieces of optical components such as mirrors, beam splitters, lenses, and gratings are integrated on a single chip of silicon, and they are electromechanically movable to redirect optical beams in a free-space. Fundamental concept of micro optical systems has been reported elsewhere [3].

Most MEMS OXCs use a pair of micro mirror arrays [4] as a switching element between the optical fiber collimators as schematically shown in Fig. 1 (a). To minimize coupling loss of optical fibers, a light beam should be coupled into the fiber in parallel with the collimator's axis. Hence each fiber has its own 2D steering, and switching is done in free-space between any arbitrary pair of such fiber-mirror units. One of the drawbacks of this architecture is considerable difficulty in aligning optical components used in the system, namely, fibers, collimators, and MEMS mirrors.

On the other hand, an equivalent but compact optical system is possible by using translating collimators as shown in Fig. 1 (b). The input fiber is placed at the focal length of the lens, and the collimated beam is steered in 2D by the translating motion of the lens [5, 6]. As there are only two optical components (fiber and lens)to be aligned in line, housing of the whole setup can be simplified. Although optical insertion loss could be large due to the additional interfaces associated with the lens scanner mechanism, we have studied this type of switching architecture for its favorable features listed in Table I. Different from the tilting mirrors [7], steering angle of translating lens is linear to the displacement of the lens, which enables us to easily predict the point of shooting. Furthermore, independent XY-scan is possible thanks to the decoupled motion of the XY-stage. While double-gimbal type 2D scanner require four sets of high-voltage analog amplifiers for 2D operation, our lens scanners need only four switching transistors, and thus the driving electronics can be simple. Lens scanners of similar mechanism using piezoelectric PZT actuators have been reported by other researchers [8]. Our approach uses surface micromachined actuators for lens translation for more integrability.

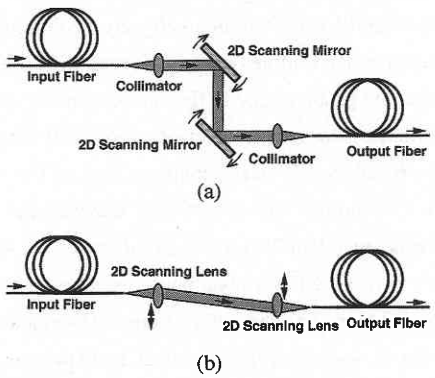

Fig. 1 (a)Free-space optical crossconnetor using a pair of 2D scanning mirrors and (b) 2D scanning lens.

*Center for International Research on MicroMechatronics, Institute of Industrial Science, University of Tokyo
**Electrical Engineering, University of California Los Angeles, CA, USA

Table I Comparison of OXC's based on (a) tilting mirror and (b) translating lens

Principle	(a) Mirror	(b) Lens
Motion	Tilt	Translation
Transfer Function	Nonlinear Large X-Y Crosstalk	Linear to translation No X-Y Crosstalk
Control	Analog Voltages (4 Op.-Amps / mirror)	Digital Switches (4 Switches / lens)
Self-Holding	Not Available	Available
Insertion Loss	Small	Large due to many interfaces

2. MEMS 2D Lens Scanner

Figure 2 illustrates the MEMS OXC using 2D lens scanner array. Fiber bundles are used for optical input and output, and 2D array of 2D lens scanners are placed in free-space between them. Each input fiber has its own transmitting lens scanner, and traveling beams are directed to any one of the lens scanners on the receiver module. In addition, the schematic shows potential use of additional macro lenses in a telescopic formation to magnify the scan angle of the traveling beams.

The platform of the 2D scanner has been fabricated by using a foundry service called MUMPs [9], and a micro lens has been post-processed by in house by using the photoresist reflow technique. Figure 3 (a) shows a part of 2x2 lens scanner array, and Fig. 3 (b) is a close-up view (lens diameter 260 microns, approximate focal length 670 microns).

In the post-process, photoresist (Hoechst AZ-4620) was first formed in a circular pattern on the MEMS XY-stage, and hard-baked at 150 degree C for 1 minute for thermal reflow. Sacrificial phosphosilicate glass (PSG) layers were removed in concentrated hydrofluoric acid (47%) for 10 minutes in a dark environment (to avoid damage to the polysilicon surface due to photovoltaic effect) followed by two cycles of careful rinse in de-ionized-water (DIW) warmed at 60 degree C for 30 minutes each. Chips were naturally dried without using any alcohol replacement. As the structures had dimples in poly1 layers, they did not suffer from the sticking problem due to the surface tension of water.

The position of the lens is electromechanically controlled by using two pairs of scratch-drive actuators (SDA) [10], as shown in Fig. 3 (b). Decoupling sliders attached between the stage and SDAs allow independent 2D motion of the stage [11]. For electrical isolation between SDA arrays, photoresist bridges are used to connect the SDA array to the ladder frame. As depicted in Fig 4, the stage plate is suspended at approximately 20 microns above the substrate by stress-induced cantilevers (made of polysilicon with evaporated chromium and gold) in order to reduce surface friction.

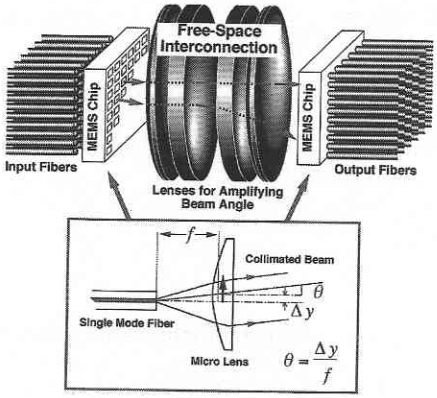

Fig. 2 Schematic view of MEMS OXC using 2 D lens scanner array. Macro lenses in telescope formation are used for magnifying the scan angle of traveling beams.

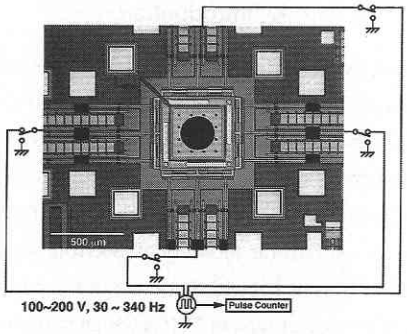

(a)

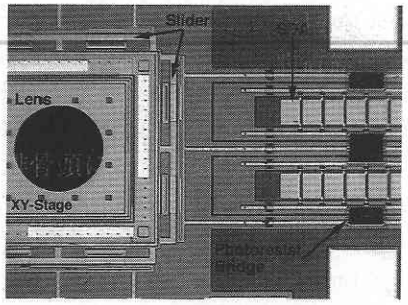

(b)

Fig. 3 Photographs of polysilicon surface micromachined 2 D lens scanner. (a) entire view and (b) close-up view of the XY-stage. The lens is made by thermally reflow photoresist.

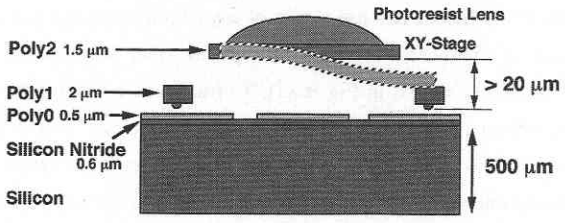

Fig. 4 Schematic cross-section of the lens scanner.

Note that the photoresist lens is backed up with a 1.5-micron-thick polysilicon plate to avoid electrostatic charge-up, which otherwise causes permanent adhesion of the lens onto the substrate.

3. Photoresist reflow lens

A photoresist before reflow has a cylindrical shape of height t and diameter D, and its volume is written

$$V_{cylinder} = \frac{\pi}{4} D^2 t. \quad \cdots\cdots (1)$$

Our experiment observed that the photoresist reflowed into a spherical shape without changing its original diameter. So we use the same D to write the volume of plano-convex lens of sag s as

$$V_{planoconvex} = \frac{\pi s}{24} (3D^2 + 4s^2). \quad \cdots\cdots (2)$$

Assuming that change of volume during thermal reflow is negligible, we equalize (1) and (2) to find the sag as

$$s = A - \frac{1}{4}\frac{D^2}{A}, \quad \cdots\cdots (3)$$

where

$$A = \frac{3}{4} t D^2 + \frac{1}{8}\sqrt{D^6 + 36 t^2 D^4}. \quad \cdots\cdots (4)$$

Radius of curvature of the lens is written

$$R = \frac{s}{2} + \frac{D^2}{8s}, \quad \cdots\cdots (5)$$

and focal length is [12]

$$f = \frac{R}{n-1}, \quad \cdots\cdots (6)$$

where n is refractive index. Substituting (5) into (6), we find the focal length as

$$f = \frac{R}{n-1}\left\{\frac{s(t,D)}{2} + \frac{D^2}{8s(t,D)}\right\}. \quad \cdots\cdots (7)$$

Therefore, focal length of a photoresist reflow lens should be controlled by the initial thickness of photoresist and the dimension of mask pattern.

As a lens material, we used double-spun Hoechst AZ-4620 at 2000 rpm for 30 seconds for an initial thickness of 23 microns. To investigate the effect of dimensions on focal length, we patterned the photoresist into circular shapes of various diameters ranging from 200 to 800 microns by photolithography and developed in diluted developer (100 ml of concentrated AZ-400K and 100 ml of DIW) for 1 minute at room temperature. They were hard-baked on a hot plate at 150 degree C for 1 minute in atmospheric environment for thermal reflow.

To evaluate the focal length of each micro lens, we directed a 1.55-micron-wavelength infrared beam diverging from a single mode fiber to the convex surface of the lens and observed a spot projected onto an infrared sensor card placed at 1 meter away. We defined the focal length by the distance between the fiber facet and the photoresist convex such that the beam was collimated and that the projected spot size was minimized. Figure 5 plots the experimentally obtained focal length of photoresist lens as a function of lens diameter. The distribution of the data points could be fairly well explained by the theoretical prediction when using the refractive index of 1.7 as a fitting parameter. We used this model to find optimal thickness of photoresist to be 10 microns for a mask pattern of 260 micron in diameter to make a micro lens of 670-micron focal length.

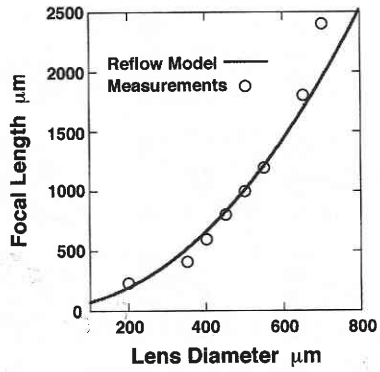

Fig. 5 Focal length of photoresist reflow lens. Experimental measurements (circles) agree very well with theoretical prediction (solid curve).

4. Beam Steering with MEMS 2D Lens Scanner

The position of the lens is controlled by counting the total number of voltage pulses applied to the scratch-drive actuators. Figure 6 shows microscope VCR clips of the 2D lens scanner in operation. Maximum traveling distance was designed to be 67 microns in the both directions, limited by the stoppers attached to the sliders' guide rails. Average number of pulses needed to travel from one end to the other was experimentally found to be 400 pulses for square voltage of 200 V at 340 Hz, corresponding to a traveling time of 1.2 seconds.

The MEMS chip was mounted and wirebonded on a printed circuit board (PCB) as shown in Fig. 7. We placed the chip in front of a fiber to observe an infrared beam steered in 2D by using an infrared CCD camera located at an 8-cm distance behind the chip as illustrated in Fig. 7 (b). For precise positioning the chip to the fiber, we employed a commercially available lens holder of five degrees of freedom ($XYZ\phi\theta$).

Figure 8 shows displaced beam spots observed with the CCD camera. Maximum spot displacement of more than+/-10 mm on the CCD image plane was obtained, corresponding to a scan angle of+/-7 degrees. Unlike electrostatic scanning mirrors or thermally driven lens scanners [13], the lens scanner can be latched at any place without power consumption. The beam spot is accompanied with several coaxial ring patterns due to the optical interference between the multiple interfaces of the MEMS stage (see Fig. 4). In

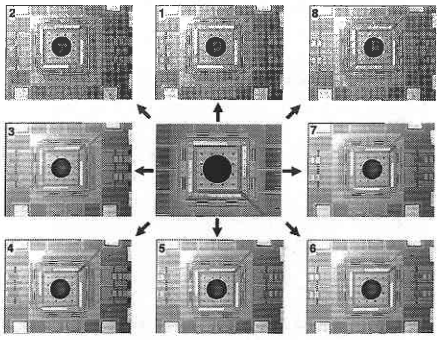

Fig. 6 Snap-shots of micro lens scanner in 2 D motion.

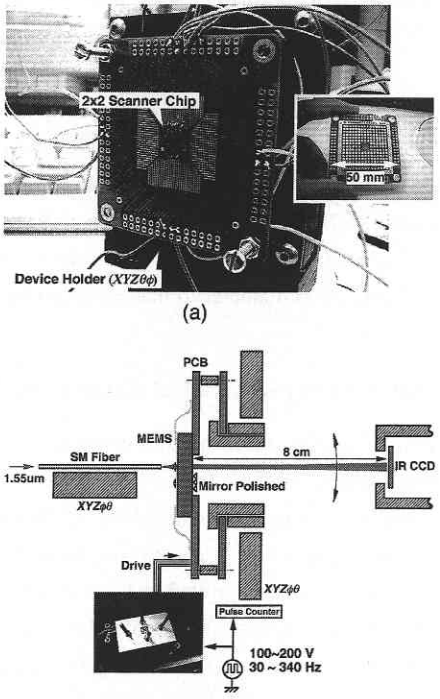

Fig. 7 (a) Micro 2 D lens scanner chip mounted and wire-bonded on a printed circuit board. (b) cross-sectional setup of optical apparatus for observing steered infrared beam.

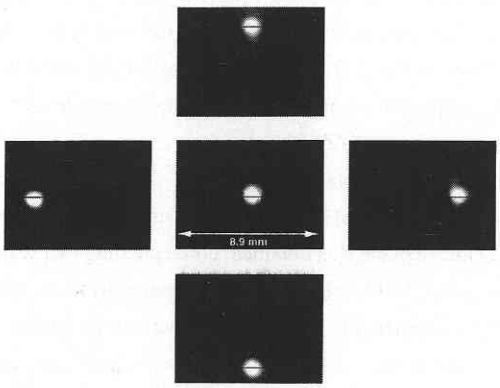

Fig. 8 Infrared CCD images of 2 D steered beam spots. Scan angle of+/-7 degrees was larger than the image plane of the CCD.

order to suppress this effect and to improve transmission efficiency, anti-reflection coating would be needed on those surfaces. Transmission loss through the substrate can be lowered by using a thinner substrate or replacing it with a transparent one by the device transplant technique [14].

5. Conclusion

In summary, microlens scanners on surface micromachined XY-stages have been successfully fabricated, and preliminary results of infrared beam steering have been demonstrated. The scanner sometimes exhibited stick-and-slip motion due to the friction between the guide rails and SDA's ladder-bars, which had been buckled by the residual stress of photoresist bridges. New designs are under development to minimize the friction problem. Post-process of photoresist reflow was performed chipwise, and thus a large edge bead of photoresist was found on the chip after spin coating. This caused distributed initial thickness of photoresist, resulting in variation of lens sag. For better reproducibility, post-processing should be performed waferwise.

(Manuscript received, December 8, 2000)

Acknowledgements

A part of this work performed at UCLA has been supported by 1998 Zaigai-Kenkyu Program of Ministry of Education, Science, Sports and Culture of Japan.

References

1) H. Fujita and H. Toshiyoshi, "Micromechanical Optical Devices," Oyo Buturi, Japan Society of Applied Physics, vol. 69, No. 11, 2000, pp. 1274–1284 (in Japanese).

2) P.Rai-Choudhury: Handbook of Microlithography, Micromachining (SPIE Optical Engineering Press, Bellingham, Washington, USA, 1997) (Refer to a contributed chapter "Chapter 8, MICRO-OPTICAL DEVICES" by H. Fujita and H. Toshiyoshi, pp. 435–516).

3) M. C. Wu, L. Fan, G.-D. Su, "Micromechanical Photonic Integrated Circuits," Trans. IEICE, vol. E83-C, No.6 (2000) p.903.

4) D. T. Neilson, V. A. Aksyuk, S. Arney, N. R. Basavanhally, K. S. Bhalla, D. J. Bishop, B. A. Boie, C. A. Bolle, J. V. Gates, A. M. Gottlieb, J. P. Hickey, N. A. Jackman, P. R. Kolodner, S. K. Korotky, B. Mikkelsen, F. Pardo, G. Raybon, R. Ruel, R. E. Scotti, T. W. Van Blarcum, L. Zhang, C. R. Giles, "Fully Provisioned 112x112 Micro-Mechanical Optical Crossconnect with 35.8Tb/s Demonstrated Capacity," Proc. 25th Optical Fiber Comm. Conf (OFC2000), Bantimore, MD, Mar. 7–10, 2000, PD12–1.

5) H. Toshiyoshi, G.-D. J. Su, J. LaCosse, M. C. Wu, "Micromechanical Lens Scanners for Fiber Optic Switches," Proc. 3rd Int'l Conf. on Micro Opto Electro Mechanical Systems (MOEMS 99), Aug. 30-Sep. 1, 1999, Mainz, Germany, pp. 165-170.

6) H. Toshiyoshi, G.-D. J. Su, J. LaCosse, M. C. Wu, "Surface Micromachined 2D Lens Scanner Array," Proc. IEEE/LEOS Optical MEMS, Kauai, Hawaii, Aug. 21-24, 2000, Late News Session, PD-1.

7) H. Toshiyoshi, W. Piyawattanametha, C. T. Chan, and M. C. Wu, "Linearization and Analysis of Electrostatically Actuated MEMS 2D Optical Scanner," Solid-State Sensor&Actuator Workshop (Hilton Head 2000), June 4–8, 2000, Hilton Head Island, SC (Supplemental Digest of Late News Poster Session), pp. 7–8.

8) S. Glockner, R. Goring, B. Gotz, A. Rose, A, "Piezoelectrically driven micro-optic fiber switches," Optical Engineering, vol. 37, (no. 4), SPIE, April 1998. pp. 1229–34.

9) See the web page of the manufacturer, http://www. memsrus. com/cronos/svcsmumps. html.

10) T. Akiyama, D. Collard, H. Fujita, "Scratch drive actuator with mechanical links for self-assembly of three-dimensional MEMS," IEEE J. Microelectromechanical Syst., vol.6, (no.1), March 1997. p. 10–17.

11) L. Fan and M. C. Wu, "Self-Assembled Micro-XYZ Stages for Moving Micro-Ball Lenses," Int. Conf. on Optical MEMS and Their Applications (MOEMS 97), Nara, Japan, November 18–21, 1997.

12) Bahaa E. A. Saleh and Malvin C. Teich: Fundamentals of Photonics (John Wiley & Sons, Inc. New York, 1991).

13) A. Tuantranont, V. M. Bright, J. Zhang, W. Zhang, J. Ness, and Y. C. Lee, "MEMS-Controllable Microlens Array for Beam Steering and Precision Alignment in Optical Interconnect System," Proc. 2000 Solid-State Sensor and Actuator Workshop (Hilton Head 2000), Hilton Head Island, SC, pp. 101–104, June 4–8, 2000.

14) H. Nguyen, J. Su, H. Toshiyoshi, and M.C. Wu, "Device Transplant of Optical MEMS for out of Plane Beam Steering," to be presented at 14th Annual IEEE International MEMS-01 Conference, January 21–25, 2001, Interlaken, Switzerland.